EFFECT OF MECHANICAL LOADING AND WATER SATURATION ON THE GAS RECOVERY OF TIGHT GAS: EXPERIMENTAL STUDY

X. Fu [1,2,3], F. Agostini [1,2,3],
L. Jeannin [4], C.A. Davy [1,2,3], F. Skoczylas [1,2,3]

1 Université Lille Nord de France, F-59000 Lille, France
2 Ecole Centrale de Lille, LML, BP 48, F-59651 Villeneuve d'Ascq, France
3 CNRS, UMR 8107, F-59651 Villeneuve d'Ascq, France
4 GDF/Suez E&P, 1 Place Samuel de Champlain, 92930 La Défense Cedex, France
Email: xiaojian.fu@ec-lille.fr

This paper was prepared for presentation at the International Symposium of the Society of Core Analysts held in Aberdeen, Scotland, UK, 27-30 August, 2012

ABSTRACT

So-called tight gas reservoirs are constituted of low permeability sandstones(less than 10^{-16} m^2 without hydrostatic loading), with a connected porosity lower than 12%, and a strong sensitivity to in-situ stresses as compared to conventional reservoirs. Focused on sandstones, this article assesses their actual petro-physical properties, namely porosity, gas permeability under varying hydrostatic stress and water saturation. Poro-mechanical measurements are carried out to highlight microstructure variation, and the observation reveals that some pores are entrapped with increase of mechanical loading.

INTRODUCTION

"Tight sandstone" is a type of "unconventional gas reservoir". Below the ground, oil, or natural gas, are trapped in ultra-compact rocks called "tight reservoir". The compactness of the rock is so elevated that the gas is not able to move easily, which means that the production of the gas reservoir is difficult.

In tight sandstone reservoirs, the gas is trapped in the rock porosity. A so called "tight sandstone" is a low permeability sandstones with sensitive petrophysical properties that may affect the productivity of the deposit [1, 2]. The intrinsic gas permeability is weak (less than 0.1 mD, videlicet 10^{-16} m², without hydrostatic loading). The connected porosity is below 12% and this kind of material exhibit a high sensitivity to in-situ stress compared to that of conventional rock reservoirs [3, 4, 5]. Moreover, a transition zone called permeability jail [2,6], which can extend over several hundred meters above the water table, is observed in situ. In a previous study carried out on sandstones provided by GDF/Suez, it was shown that, for a range of saturation from 40 to 50%, gas was not mobile enough for industrial extraction [7].

This study aims at characterize the factors influencing gas permeability of sandstone, such as mechanical loading (through the use of different confining pressures) and physical of rocks (porosity), and water saturation; on the other hand, to evaluate the changes in sandstone microstructure, variation of pore volume and compression modulus, under different confining pressures, will be the main tools. Sensitivity to external stress is correlated with sandstone microstructure changes under stress using poro-mechanical experiments [8].

CHARACTERIZATION AND EXPERIMENTAL METHODS

This section details the different experimental protocols to characterize the sample gas permeability, and its main poro-mechanical properties.

Experimental Methods For Porosity And Saturation Measurements

The different sample mineralogical composition is mainly silica and a variable amount of clays. The cementation of the silica grains is variable among different samples. They were drilled from 4836.45 m to 5013.61 m of depth.

Connected porosity (φ) and initial water saturation ($S_{w,ini}$), have been firstly measured. The "as received" mass, designated as initial mass (m_{ini}) is measured. Secondly, samples are placed in an oven at 60°C until weight stabilization (mass variation lower than 0.01g between two successive weighing separated by 1 week) to determine the dry mass (m_{dry}). A balance with a precision of 0.01g was used for this purpose. Re-saturation in water (in vacuum) at 20°C allows the measurement of the fully saturated mass (m_{sat}) (same criterion for mass stabilization).

The values of porosities measured and initial saturations are presented in Table 1.

Table 1. *Porosity and initial saturation of tight sandstone samples*

Number	505	225	2425	2925	765	1655	2775	1495	1335	585	55	2015	185	1073
Porosity (%)	6.4	2.5	6.8	11.9	7.2	7.0	7.1	8.5	6.4	6.1	5.3	7.7	-	-
$S_{w,ini}$ (%)	12	24.3	21.3	16.8	19.6	15.2	20.7	13.5	26	17.6	43.3	20.5	-	-

Note: the symbol "–" signify that this item was not determined

The porosities stand between 2.5% and 12%, and the initial saturations cover a range between 12.0% and 43.3%.

Methodology For Obtaining A Homogeneous Saturation

To study the influence of water saturation on gas permeability, a series of saturation values were obtained by the method of over-saturated salt solutions. After full saturation at 20 °C, each sample was placed into a desiccator in which a brine solution provides a given relative humidity (RH). After a period of time (about 60 days), the mass stabilizes, and the material reaches a homogenous water saturation.

This technique is generally used to scan a wide range of saturations and to obtain isotherm sorption/desorption curves. Due to the pore size of material, this method does not allow to obtain saturations higher than 62% (see section 3.3).

Experimental Method For Measuring The Porosity According To Confining Pressure

To estimate variation of porosity according to confining pressure, a buffer tank and a hydrostatic cell are used as a closed system [8] (Figure 1). Gas pressure (P_1) is set up in the buffer tank of known volume (V_1).

After the stabilization of both confining pressure (Pc) and pressure (P_1) in the buffer tank, the gas is released in the sample which is on dry state. Gas pressure in the buffer tank decreases to P_2. The volume V_2 at pressure P_2 is the sum of the pore volume of the sample (V_{pore}), the volume of the buffer tank (V_1) and the volume of the tube between the sample and the buffer tank ($V_{extinct}$).

Assuming that the gas is ideal under isothermal conditions (Eq. (1)), the pore volume, under confining pressure, can be calculated by the use of equation (2):

$$P_1V_1 = P_2V_2 \quad (1)$$

$$V_{pore} = V_2 - V_1 - V_{extinct} \quad (2)$$

A succession of measurements is then carried out with different values of confining pressures, which provides the variation of the porosity according to this pressure.

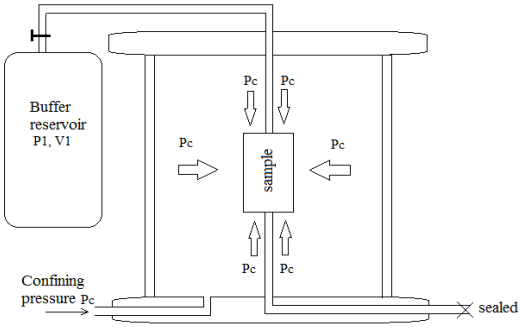

Figure 1. *Experimental cell for the measurement of porosity – confining pressure*

Experimental Method For Poro-Mechanical Test

Poro-elastic properties [9] are identified by measuring volumetric strains under increasing confinement. Prior to being placed inside a triaxial cell, the sample is equipped with two longitudinal and two transversal strain gauges ((ε_1, ε_2), and (ε_3, ε_4) respectively), all placed at mid-height. Volumetric strain is deduced using the hypothesis of an isotropic medium [7] by:

$$\varepsilon_v = \frac{3(\varepsilon_1+\varepsilon_2+\varepsilon_3+\varepsilon_4)}{4} \quad (3)$$

By definition, when considering a homogeneous, isotropic porous medium under constant pore pressure p and subjected to a variation in hydrostatic stress $\Delta\sigma_H=\Delta P_c$, drained bulk modulus K_b [10, 11] is given by [9]:

$$K_b = \frac{\Delta P_c}{\Delta\varepsilon_{v1}} \quad (4)$$

where $\Delta\varepsilon_{v1}$ is the volumetric strain variation due to hydrostatic stress variation ΔP_c. K_b is deduced from Eq. (4), as the slope of the linear interpolation of the stress-strain curve (ε_v,P_c) during an unloading phase of ΔP_c = 5MPa: it is therefore a secant bulk modulus K_b. When assuming that such a limited unloading only releases elastic energy, determining K_b is bound to be performed in the elastic domain. Moreover, the sample is drained freely at both ends while confining pressure is increased or decreased: p remains equal to atmospheric pressure P_{atm} (zero relative pressure) during all tests. Drained modulus K_b provides an evaluation of the solid skeleton deformability: K_b accounts for the deformability of:

a) the solid skeleton, which, for sandstones, is mainly composed of cemented silica grains, mixed with varied solid phases in smaller amounts;

b) the connected and non connected pore networks.

Poro-mechanical test is also used to measure the solid matrix bulk modulus K_s, which represents the solid matrix rigidity: it is obtained from volumetric strain variation when the porous medium is subjected to $\Delta p = \Delta Pc$, as:

$$K_s = \frac{(\Delta p = \Delta P_c)}{\Delta\varepsilon_v} \quad (5)$$

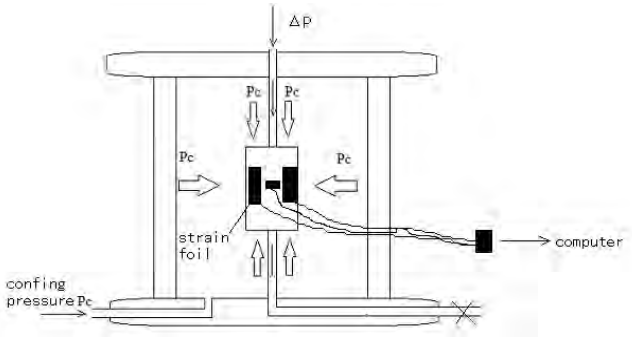

Figure 2. *Experimental cell for poro-mechanics*

FACTORS INFLUENCING GAS PERMEABILITY

For gas reservoirs rocks, the permeability is a major characteristic. This study aims to highlight the influence of three factors, analyzed in the following sections: porosity, confining pressure and water saturation. The gas permeability is measured by the experimental method called "transient pulse test technique" [12, 13, 14]. Permeability values presented in this article are actually apparent permeability. Indeed, the same gas injection pressure has been used for all the measures. As a consequence, Klinkenberg or Forchheimer effects have not been taken into account.

Influence Of Porosity On The Gas Permeability

Figure 3 shows the dry permeability of the samples measured at dry state (Sw = 0), under varying confining pressure. Thus, each sample refers to a porosity value (see Table 1).

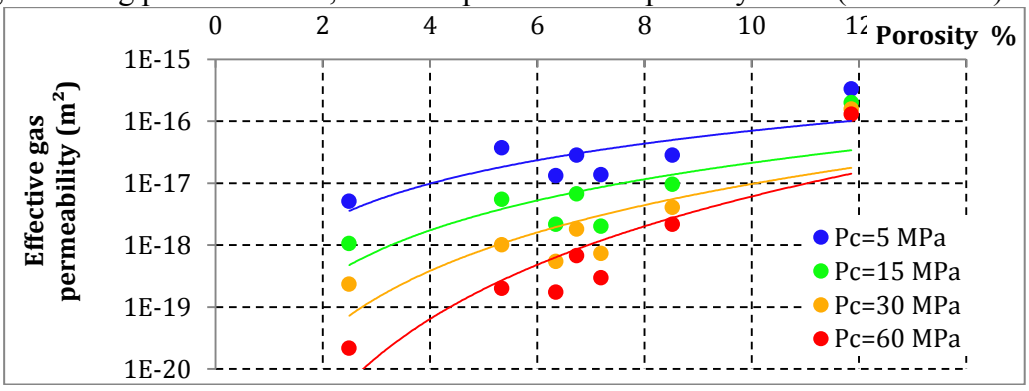

Figure 3. *Influence of porosity on effective gas permeability (1 m² = 1E15 mDarcy)*

The results show a similar trend for all the imposed confining pressure. A higher porosity is related to a higher permeability. It can also been observed that the sensitivity to confining

pressure increases when porosity decreases. For 2.5% porosity, effective gas permeability is divided by more than 200, while it is divided by 13 for a porosity of 8.5%, when confining pressure is raised from 5 to 60 MPa. For 12% of porosity it is only divided by 2. This can be a sign of micro cracking, closed by mechanical loading.

Influence Of Confining Pressure On Gas Permeability

The influence of confining pressure is shown in Figure 4 which gives the results of effective permeability of the samples at their initial saturation ($S_{w,ini}$). For each sample, the permeability is measured over a range of confining pressures from 5 MPa to 60 MPa.

Figure 4 shows that the permeability decreases with increasing confining pressure. This trend is identical for all samples and is also found in the literature [7, 12]. The permeability loses (at least) 1 order of magnitude between 5 and 60 MPa of confinement, which is also the mark of a cracking of the material.

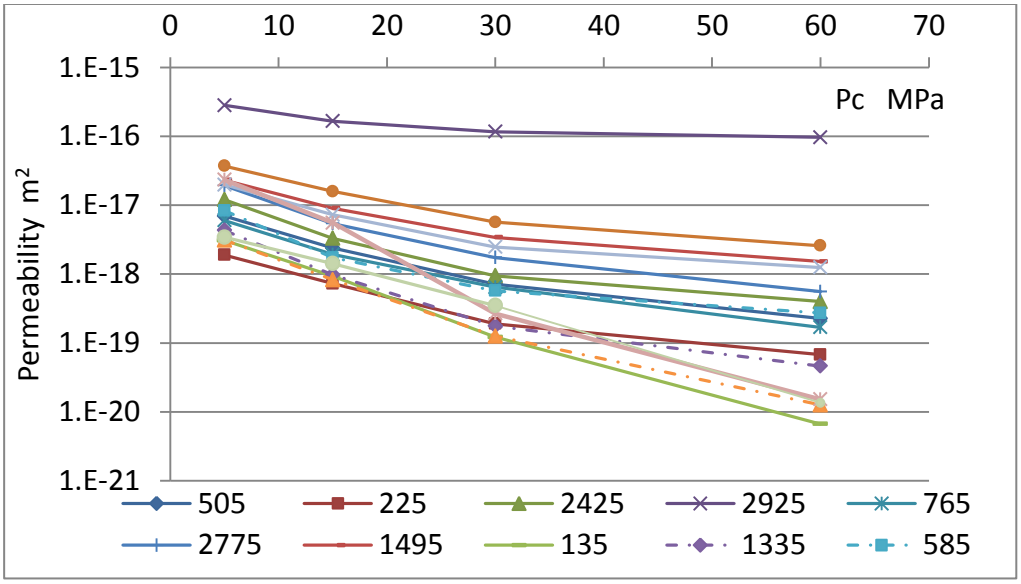

Figure 4. *Gas permeability variation according to confining pressure (initial state of saturation)*

Influence Of Water Saturation On The Gas Permeability

Gas permeability analysis according to water saturation was performed on samples at either initial saturation or at saturation obtained by the method of over-saturated brine solutions. Having no sorption data on tight sandstone, it is impossible to know by advance the saturation value which will be obtained using a given relative humidity. This first section presents the relationship between imposed capillary pressures (calculated from imposed relative humidity)

and saturations obtained by the method of brine solutions. The second section details the influence of saturation on the gas permeability.

Saturations Obtained By The Method Of Over-Saturated Brine Solutions

Figure 5 shows the relationship between capillary pressure and liquid saturation. This curve is known as being the characteristic curve. Capillary pressure is calculated from the relative humidity according to Kelvin's law:

$$p_{cap} = \frac{\rho_w RT \ln(RH)}{M_w} \quad (6)$$

In which P_{cap} is the capillary pressure (Pa); ρ_w is the density of liquid water (kg/m^3), R is the perfect gas constant (J/mol)； T is the absolute temperature (K)； RH is relative humidity($0 \leq RH \leq 1$); M_w is the molar mass of water (kg/mol).

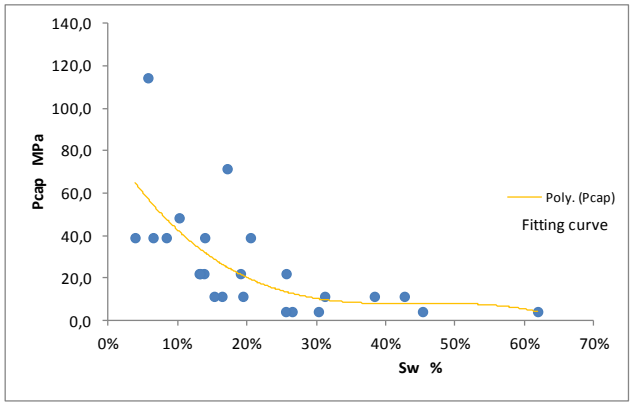

Figure 5. Saturations obtained by isotherm adsorption method

Figure 5 shows a fast decrease of water saturation with increasing capillary pressure. This traduces a contrasted pore size distribution. For a RH of 98% which gives a capillary pressure of 2.73 MPa according to Kelvin's law (Equation 6, T = 20 °C), samples exhibit water saturation ranging from 25% to 62%. And for a P_{cap} of 2.73 MPa, the corresponding de-saturated pore radius (according to Kelvin Laplace's law) is equal to 53 nm. Then we can deduce that an important part of the pore volume (38% to 75%) is constituted of large pores having a pore radius higher than 53nm. This has been confirmed through Mercury Intrusion Porosimetry measurements. This explains why it is difficult to obtain high liquid saturation (above 62%) using the over saturated brine solutions method. Furthermore, for the same P_{cap} value, there is a wide variation of obtained water saturation. This indicates a strong heterogeneity in sample pore structure.

For each saturation value, a gas permeability measurement is performed. In the next section, the influence of saturation on permeability is examined.

Influence Of Water Saturation On Gas Permeability

Figure 6 shows the gas relative permeabilities of tight gas samples, according to the water saturation, for a confining pressure equal to 5 MPa.

Changes in gas relative permeability show firstly a sharp decrease with increasing saturation. This trend was also observed for other sandstones; see for example [12]. This is due to the increase in the amount of free water present in the porosity of the material, which makes the gas passage more difficult.

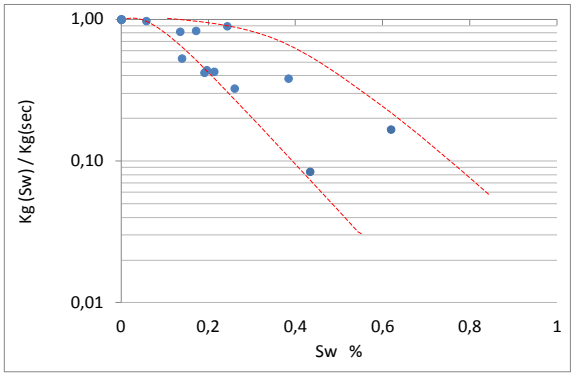

Figure 6. Gas relative permeability according to water saturation

In the case of tight gas, a hydraulic cut-off may appear when both water saturation and mechanical loading increase. This has been detailed in previous study [2, 7].

PORO-MECHANICAL BEHAVIORS

Variation Of Porosity With Confining Pressure

The total volumetric strain ε_v is due to the variation of pore volume $\Delta\varphi$ and to the matrix volumetric strain ε_{vo} [9];

$$\varepsilon_v=\Delta\varphi + \varepsilon_{vo}.(1-\varphi) \quad (7)$$

Relation (7) allows detecting pore trapping or cracking closure with increasing confining pressure, using the experimental apparatus combined from the unit presented in Figure 1 and Figure 2. The confining pressure is progressively increased. ε_v is monitored using strain gages. Punctual gas injection into the sample allows the evaluation of porosity changes.

Figure 7 presents the results of variation (in %) of porosity (compared with initial porosity) and volumic strain (in %).

As it can be seen in Figure 6, we can see that $\Delta\varphi > \varepsilon_v$. This proves that pores are entrapped into the matrix. This is due to micro-cracks closure.

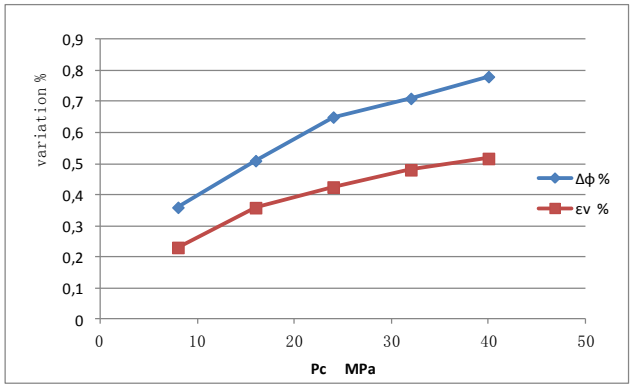

Figure 7. Variation of porosity and the volumetric strain versus confining pressure

Poro-Mechanical Measurement

The cell presented in Figure 2 is used to carry out poro-mechanical tests [7]. The results are presented in Figure 8.

Poro-mechanical tests have been performed on tight gas sample. The variation of both Kb and Ks with mechanical loading is presented in Figure 8 for one sample.

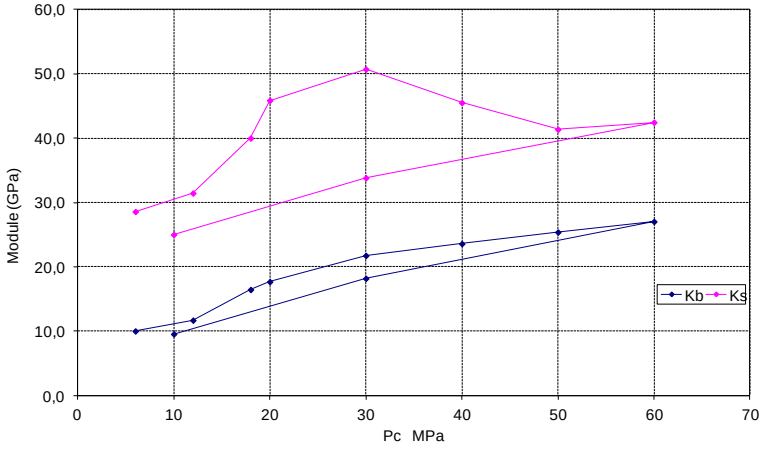

Figure 8. Poro-mechanical study of one sandstone sample

With increasing confinement, Kb increases almost linearly. Ks is an apparent modulus, in the sense that it reflects the incompressibility of the solid skeleton, but also the unconnected porosity [2]. The variation of Ks with confining pressure along with the variation of porosity (Figure 8) leads to the following interpretation. In a first stage, when mechanical loading increases, some pores are closed as represented in Figure 9 (a). Secondly, if the closure of cracks encircle a pore (Figure 9 (b)), both Ks modulus and accessible porosity are lowered.

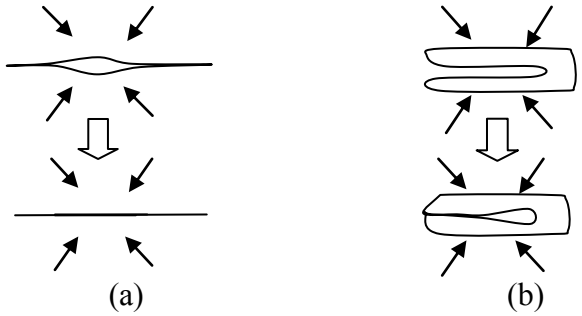

Figure 9. Variation of crack under confining pressure

CONCLUSIONS

In the context of unconventional reservoirs like "tight sandstone", the permeability of the rock is a critical characteristic for the industrial extraction of natural gas. This study deals with the influence of three parameters on the evolution of the gas permeability of tight sandstone. More detailed findings are highlighted below.

The microstructure and the pore structure of tight sandstones are highly heterogeneous in terms of their drilling depth. The studied samples do not exhibit the same initial saturation and porosity.

The mechanical environment, reproduced in our study through confining pressure, induces a decrease in gas permeability with increasing pressure. This is explained by the decrease of pore volume with increasing confining pressure, which complicates the flow of gas into the pores of the material and closing of cracks.

The porosity of the material influences the gas permeability: the higher the porosity, the higher the gas permeability. The influence of mechanical loading is reduced with increasing porosity, confirming the presence of crack.

To study the variation of microstructure with mechanical loading, poro-mechanical tests coupled with accessible porosity measurements have been performed. The result shows that when confining pressure increases, the apparent porosity of the sandstone sample decreases,

linked to a decrease of solid matrix bulk modulus. This has been explained by the trapping of pores in the solid matrix.

REFERENCES

[1] Shanley K.W., Cluff R. M. and Robinson J. W., Factors controlling prolific gas production from low-permeability sandstone reservoirs: Implications for resource assessment, prospect development, and risk analysis. *AAPG Bulletin*, 2004, 88(8): 1083-1121.

[2] FU X., F. Brue, F. Agostini, L. Jeannin, C.A. Davy, F. Skoczylas, Influence de la pression de confinement, de la porosité et de la saturation sur la perméabilité au gaz des grès tight, *Transfert 2012*, 2012, S4-5: 231-240.

[3] Ward J.S., Morrow N. R., Capillary Pressures and Gas Relative Permeabilities of Low-Permeability Sandstone. *SPE Formation Evaluation*, 1987, SPE 13882, 345-356.

[4] Chowdiah P., Effects of Pore Water Distribution and Stress on the Laboratory Measurement of Tight Sandstone Properties. *SPE Formation Evaluation*, 1986, SPE 15210, 35-46.

[5] Luffel D.L., Howard W. E. and Hunt E.R., Travis Peak Core Permeability and Porosity Relationships at Reservoir Stress, *SPE Formation Evaluation*, 1991, SPE19008, 310-321.

[6] Rushing J.A., Newsham K.E. and Blasingame T.A., Rock Typing - Keys to Understanding Productivity in Tight Gas Sands. *SPE Formation Evaluation*, 2008, SPE 114164, 1-31.

[7] Jeannin L., Davy. C. A, Skoczylas. F.,Portier. E., Fu. X., Agostini. F., Hydraulic cut-off and gas recovery potential of sandstones from tight gas reservoirs: a Laboratory Investigation. *45th U.S. Rock Mechanics / Geomechanics Symposium*, 2011, 11-348.

[8] Chen X.T., Davy C.A., Skoczylas F. and Shao J.F., Effect of heat-treatment and hydrostatic loading upon the poro-elastic properties of a mortar, *Cem. Concr. Res*, 2009*,* 39 195-205.

[9] Coussy O., *Poromechanics*, J. Wiley & Sons, New York, 2004.

[10] A. Nur and J. D. Byerlee, An exact effective stress law for elastic deformation of rock with fluids. *Journal of Geophycal Reserch*, 76(26): 6414–6419.

[11] F. J. Ulm, G. Constantinides, and F. H. Heukamp. Is concrete a poromechanics materials? A multiscale investigation of poroelastic properties. *Materials and Structures / Concrete Science and Engineering*, 2004, 37: 43–58.

[12] Dana E, Skoczylas F., Gas relative permeability and pore structure of sandstones. Int *J Rock Mech Min Sci*., 1999, 36: 613–625.

[13] Davy C. A., Skoczylas F., Barnichon J.-D. and Lebon P., Permeability of macro-cracked argillite under confinement: Gas and water testing. *Phys. Chem. Earth (A)*, 2007, 32: 667–680.

[14] Lion M., Skoczylas F. and Ledésert B., Determination of the main hydraulic and poro-elastic properties of a limestone from Bourgogne, France. *Int J Rock Mech Min Sci*, 2004, 41: 915–925.